

Generating Multi-Sensor Precipitation Estimates over Radar Gap Areas

SHAYESTEH E. MAHANI and REZA KHANBILVARDI

Civil Engineering Department

City University of New York (CUNY) &

Cooperative Remote Sensing Science and Technology (NOAA-CREST) Center

160 Convent Ave., New York, NY, 10031,

USA

mahani@ce.ccny.cuny.edu

Abstract: Generating a multi-sensor precipitation product over radar gap area is the objective of the present study. A merging approach is developed to improve Satellite-based Precipitation Estimates (SPE) by merging with ground-based Radar Rainfall (RR) estimates because remote satellites are the only source that can collect information from areas where are inaccessible by ground-based radar and/or rain gauge networks. The merging algorithm is capable of extending radar information from pixels with available RR to their neighboring pixels with no radar information by merging RR with SPE, which is, usually, available for all pixels. SPE is combined with RR using the weighting-based approach of Successive Correction Method (SCM) after local bias correction of SPE with respect to RR. High resolution satellite infrared-based rainfall estimates from the NESDIS Hydro Estimator algorithm (HE), at hourly 4 km × 4 km basis, is selected to be merged with radar-based NEXRAD Stage IV rainfall measurements to generate rainfall product for the radar gap areas. To be able to validate the generated rainfall against NEXRAD, different size areas with available radar rainfall are selected as radar gap regions. The developed merging technique is evaluated for several study cases in summer 2003 and 2004. The results show that generated rainfall for the radar gap areas are more correlated with RR (average 0.67) than original HE with RR (average 0.36) and the RMSE between merged and radar rainfall (average 2.8 mm) is less than the RMSE between satellite and radar rainfall (average 4.48 mm). And also, the pattern and intensity of the generated rainfall for radar gap area became more similar to the pattern and value of RR. In addition, the enhancement of the generated rainfall with respect to RR is more significant for high rainfall amounts.

Key-Words: Merging, Radar, Gap area, Precipitation, SCM, Satellite, Rainfall.

1 Introduction:

Estimation of accurate intensity and distribution of high resolution rainfall is still a challenging effort. Rainfall intensity can be captured through different ground and remote sources of observation, such as: gauge, radar, and satellite. There is still no source of observation or a technique that can provide the realistic spatial distribution and true intensity of precipitation. In addition to observation error and instrument noise, traditional ground-based radar and gauge observations typically have limited spatial coverage. Reliable direct rainfall information can be obtained, only, from rain gauges but at point scale, where ground-based radar system can provide indirect areal rainfall estimates at high temporal resolution. But the scanning radar beams leave many gaps in spatial coverage, particularly, over the mountainous regions, where there is heavier rainfall and snowfall, due to radar beam blockage effects.

Therefore, a more effective observing technique and source is required to cover regions where cannot be covered by ground-based rain gauge and radar systems. Satellites from remote sources are the only observation sources, capable of providing unique information about spatial distribution and intensity of precipitation from regions where are inaccessible by ground-based radar and/or gauge techniques. Satellite-based Precipitation Estimate (SPE) is indirect rainfall retrieval from visible, Infrared (IR), and/or Microwave (MW) based information of cloud properties, with larger uncertainties. Merging multi-sources products is a challenge effort for reducing some of the uncertainties and limitations associated with each source of data. There are good number of research scientists who are working on evaluating various precipitation retrieval algorithms and techniques, particularly SPE related models, to be able to understand their relevant error sources

and find solutions to enhance the accuracy of their products. Thus, using combination of multi-sensor precipitation estimates is the best solution for reducing sources of noises, instrumental errors, and minimizing bias to produce precipitation more compatible with Radar Rainfall (RR) for gap areas if it could be available. Various sizes of gap sites are selected in the areas with available RR to be able to evaluate generated multi-sensor rainfall product for. The weighting-based technique of Successive Correction Method (SCM) is used to merge SPE, which is available for all pixels, with available RR measurements for neighboring pixels of gap areas to enhance SPE data for gap pixels. The proposed merging technique is capable of extending the distribution patterns and amounts of rainfall from outside into the radar gap regions. Therefore, the developed model is efficient in generating data, more similar to RR than SPE over areas where only remotely sensed information is available.

In the present study, satellite-IR based rainfall estimates from the Hydro-Estimator (HE) algorithm is used to be improved for gap areas by merging with radar-based rainfall from the NEXRAD Stage-IV product, at hourly time and 4 km space scales. Hydro-Estimator is the modified version of the Auto-Estimator (AE) algorithm, developed, [13], at National Environmental Satellite Data and Information Service (NESDIS). High resolution HE precipitation estimates are obtained from cloud-top brightness temperature (T_b), captured by Geostationary Operational Environmental Satellite (GOES) infrared channel-4 with wavelength of 10.7 μm , along with relative humidity and precipitable water for adjusting the rainfall rates for sub-cloud evaporation, temperature and dew point profiles from North American Model (NAM) model, and topography of the interest pixel as well as its neighboring pixels. The high resolution HE products and RR information are at the Hydrologic Rainfall Analysis Project (HRAP) system with hourly 4 km \times 4 km time and spatial scales. There are efforts to validate the Hydro-Estimator rainfall products and try to improve HE algorithm [3], [7] because it is an operational rainfall retrieval model for producing high resolution SPE at National Weather Service (NWS) of the United States of America. In this manuscript, HE, from the Hydro-Estimator model, and NEXRAD Stage-IV rainfall product, are used for SPE and RR, respectively. To investigate capability of the SCM-based merging approach for producing more accurate rainfall a study area is selected in the western United States, where there are many and large radar gap areas. In order to be able to validate the accuracy of generated rainfall

for regions with no radar information, some parts of the study site with available RR are assumed to be radar gap areas. Several warm season rainfall for the months of July and August of years 2003 and 2004 have been selected for this study.

Most efforts on using multi-sensor information are only for producing more accurate Quantitative Precipitation Estimates (QPE) and also forecast (QPF) by calibrating or merging radar- and satellite-based rainfall with rain gauge observations [9] and [12] not for filling the radar gap areas. Rain gauge observations are usually assumed to be the true values of point-based rainfall amounts. SPE, after bias correction with respect to the rain gauge data, is integrated with rain gauge and radar at the National Weather Service Office of Hydrologic Development (NWS-OHD) to fill the radar gap areas and create a radar mosaic algorithm to be implemented in the quantitative Multi-sensor Precipitation Estimation (MPE) algorithm [4]. The MPE algorithm, replaces RR measurements with SPE data where RR is unavailable. The method that is used for bias correction in MPE approach is similar to the one used for combining radar with rain gauge data [4], [10], [11]. Similar multi-sensor merging approach was used for estimating more accurate stratiform rainfall in Arizona [2] with the consistent results. Satellite-based retrieved rainfall, after bias correction against rain gauge observation, was integrated with radar and rain gauge rainfall into the NWS-AWIPS [1] SIMAR program, with the goal of merging satellite, radar, and gauge information to produce one field rainfall (volume 3) product for South Africa, was developed [8]. Kriging technique was used in the merging approach of the SIMAR program to interpolate optimal rain-fields between rain gauge locations for converting point based rain gauge observations to areal-based watershed scale. The merging algorithm that was developed at the City University of New York based on the weighting approach, SCM is viable of improving satellite IR-based rainfall products by combining with radar and rain gauge information [5]. The NWS-MPE merging algorithm has been modified to enable automatic incorporation of satellite-based estimates in areas that are poorly covered by either gauges or radar. But, the proposed SCM-based merging approach is capable of generating gridded areal precipitation over the radar gap areas, more accurate than SPE, by merging SPE with RR. This approach actually extends radar-based precipitation distribution from outside inside the radar gap area, [6].

2 Methodology

The multi-sensor SCM-based merging algorithm estimates rainfall amount for every pixel, using available information from its surrounding pixels, located in a selected window, and applying weighting factors on a window base analysis. For a given pixel, located at the center of the merging window, optimum weight is calculated considering the availability of SPE and RR data as well as the distance between the center pixel and the neighboring pixels from the merging window. The window size is varied according to the size of radar gap area and the number of corresponding rainy pixels. In the present study, rainfall is produced by merging SPE with RR for areas where only RR is available. Combining merged satellite- and radar-based rainfall estimates with ground truth rain gauge observations will enhance the multi-sensor rainfall product for areas with missing rainfall observation. SCM, the weighting-based, approach is a fitting technique that makes successive correction. Before applying the proposed merging technique for quantitative integration of multi-sensor rainfall products, local bias between data needs to be corrected particularly when the objective is improving available SPE for gap areas with no ground-based information.

2.1 Local bias Correction:

Local bias is computed by comparing available SPE and RR inside a window box with different sizes from $5^\circ \times 5^\circ$ to $8^\circ \times 8^\circ$ degrees due to the size of rainy areas and spatial resolution of data. For local

bias correction of SPE with respect to RR the method that is used in the NWS-MPE model is applied for all study cases. In this model, the ratio between the rain gauge mean values and the radar mean values within a circular window is interpolated to the entire analysis domain for local bias correction of RR data [10], [11]. In most of the study cases, the SPE after bias correction, using only the ratio between mean of RR to the mean of SPE, was underestimated, particularly, for large rainfall values and was overestimated for others (Fig. 1-c). The reason, for underestimation of large amount of SPE after bias correction is probably because of a larger number of samples with smaller rainfall amounts. In the present study, the local bias was estimated by comparing the maximum as well as the mean values of the SPE and RR for corresponding rainy pixels in the selected local window box. The difference between using the mean ratio and using the mean & maximum ratios are illustrated in Figure 1-d.

For the study case that is shown in Figure 1, the mean ratio between SPE-HE and RR is:

$$r_{mean} = \text{mean}(RR) / \text{mean}(HE) = 1.1 > 1$$

and the average ratios between RR and HE mean and maximum values is about: $r_{mean \& max} = 0.65 < 1$. Only rainy pixels of RR and SPE-HE, inside the selected window box, are used to compute these ratios. Comparing figures 1-c and 1-d, which are HE after bias correction using mean ratio and mean-max ratio, respectively, with original SPE (HE before bias correction), figure 1-b, and RR, figure 1-a demonstrates more improvement using mean-max ratio for bias correction.

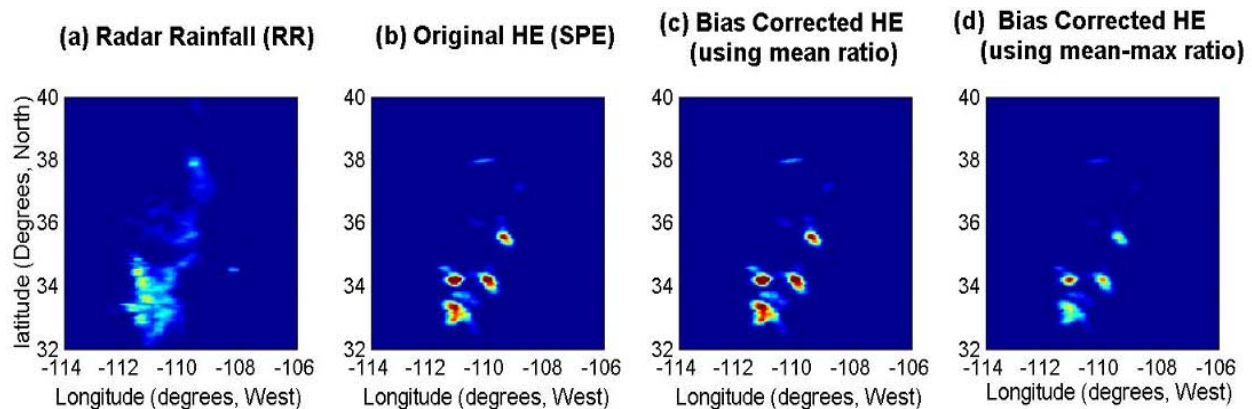


Fig. 1 Comparison between original SPE-HE before (b) and after bias correction using the ratio between radar and HE mean values (c) and using the average ratios of mean and maximum values (d). These figures show that using the mean and max ratio works better than using the mean ratio.

2.2 Merging Approach (SCM)

The next step is applying the SCM-based multi-sensor merging algorithm to enhance SPE, after bias correction, with respect to RR. The results of this study indicate that the weighting-based SCM is capable of generating merged rainfall product with minimal bias that is better suited and match with RR and has mostly the RR characteristics. The concepts of SCM merging algorithm is explained briefly in this manuscript. The details of the proposed technique have been discussed in [5].

The SCM-based model is a weighting-based approach that adjusts SPE value for any given gap pixel based on an appropriate weight for with respect to available SPE and RR information of its neighboring pixels. SPE is adjusted for the pixels that locate at the center of the selected merging window. Therefore the merging window needs to be moved around the area the way that pixels with missing data locate at the center of the window one by one. Moving the merging window from outside toward inside the gap area can extend precipitation information from outside into the gap area. In the present study, the merging window is moved in 2 positive and negative directions of each of X and Y axes to extend precipitation patterns inside the gap areas from 4 directions. The average of four adjusted SPE values is considered as the best enhanced/adjusted SPE value for each missing pixel. The size of merging window is associated with the size of the area with no RR data, size of storm, and spatial resolution of available data. In this study, various merging window sizes from 3×3 to 19×19 are used for different case studies. And for any study case, the most appropriate window size is selected by minimizing the errors of RR – adjusted-SPE for the pixels with available SPE and RR, both. SPE from Hydro-Estimator model (HE) and RR from NEXRAD Stage-IV build the two-dimensional domain for SCM in the present study. The observation error is assumed to be only a function of instrumental error/noises that is also assumed to be zero.

- The weight factor that is a function of distance between the center pixel (k) of the merging window and any other pixel (i) and the size of merging window is calculated using the formula (1):

$$\text{If } r_i < R \Rightarrow w_i = \frac{R^2 - r_i^2}{R^2 + r_i^2},$$

$$\text{and if } r_i \geq R \Rightarrow w_i = 0 \quad (1)$$

where: “ w_i ” is the weight factor related to any observation pixel (i), with available both satellite and radar rainfall amounts; “ R ” is the maximum distance from window center, pixel (k); and “ r ” is the distance between analysis center grid, pixel (k), and the observation pixel (i) inside the window, equation (2). If (x,y) are the grid pixel coordinates, then:

$$r^2 = (x_i - x_k)^2 + (y_i - y_k)^2 \quad (2)$$

- The merged/adjusted value for the center pixel (k), is calculated using the following equation (3):

$$f_{MR_k} = f_{SR_k} + \frac{\sum_{i=1}^n w_i (f_{RR_i} - f_{SR_i})}{\sum_{i=1}^n w_i + \varepsilon_{RR}^2} \quad (3)$$

where: $f_{MR(k)}$ and $f_{SR(k)}$ are the analyzed merged and satellite-based rainfall estimates for the center pixel (k), $f_{SR(i)}$ and $f_{RR(i)}$ are the satellite-based rainfall and radar rainfall for observation pixel (i) inside the window, “ n ” is the number of observation pixels with both radar and satellite rainfall estimates inside the window, and ε_{RR} is the WSR-88D (radar observation instrument) error that is assumed to be zero ($\varepsilon_{RR} = 0$).

2.3 Case Studies:

Several case studies were selected for merging SPE-HE with radar rainfall at hourly $4 \text{ km} \times 4 \text{ km}$ resolutions, using a merging window with various sizes, from 3×3 to 19×19 pixels. Areas with different sizes: $0.8^\circ \times 0.8^\circ$, $1.5^\circ \times 1.5^\circ$, and $2^\circ \times 2^\circ$ are selected over a study region in the western United States with available RR data. The selected areas are assumed to be radar gap sites. Therefore the adjusted SPE that generates for these areas can be validated using available RR measurements as independent information because they are not used for merging with or adjusting SPE. Only RR values of neighboring pixels of missing ones located outside of the gap areas are used to minimize bias of the generated rainfall. In the merging process, the generated rainfall values were also used along with available rainfall data for the pixels within the merging window to estimate rainfall for every pixel with missing RR. In the case study adjusting SPE for missing radar coverage, no iteration is applied to prevent the forcing of SPE pattern and amount to the generated rainfall over the gap area.

3 Results and Discussions

The results of applying the developed SCM-based merging technique using a merging window with different sizes to merge/adjust HE data with respect to RR for various size of gap areas demonstrated and discussed in this section. Eighteen rainy hours during July and August 2003, and fifteen rainy hours on two days: July 14th and August 15th 2004, were selected for generating rainfall over a gap region.

First, local bias of HE rainfall intensity was corrected with respect to the RR by multiplying HE

estimates to the average ratios of mean, median, and maximum of RR divided by mean and maximum of HE estimates respectively (Figure 2-a and 2-b). Figure 2 illustrates the quantity of rainfall intensity from HE algorithm before (Figure 2-a) and after bias correction (Figure 2-b) with RR (Figure 2-c), for July 14, 2004 at hour 03:00 UTC, as one example. Comparison of HE before and after bias correction with RR shows improvement of HE estimates after bias correction.

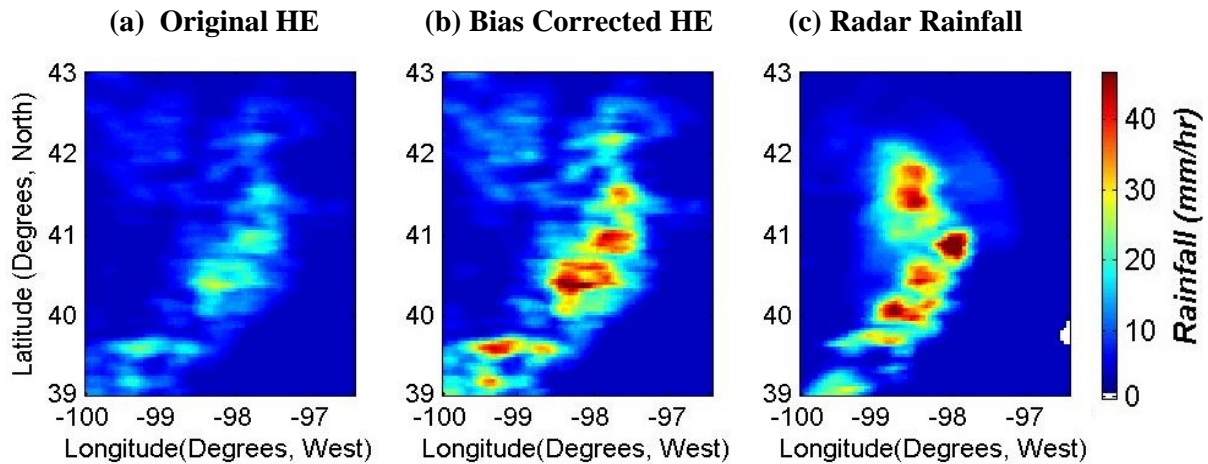


Fig. 2 Images of original HE rainfall estimates before (a) and after local bias correction (b) with respect to RR (c) for the hour 03:00 UTC on July 14, 2004. Enhancement of HE after bias correction is obvious.

A gap area was selected over a region with available radar-based rainfall data to be able to evaluate the generated merged rainfall estimates for radar missing pixels using true RR measurements. An area with different sizes of: $0.8^\circ \times 0.8^\circ$, $1.5^\circ \times 1.5^\circ$, and $2^\circ \times 2^\circ$, was created, as radar gap coverage, over the rainy part of the study site. Most radar gap areas were selected so that a good number of rainy pixels are located inside as well as outside of them. One of the created gap area, with size of $1.5^\circ \times 1.5^\circ$, on the RR image is shown in white on the Figure 3, as an example. Different size gap areas are selected over the rainy parts of the study site to determine the most reasonable merging window size for different size gap areas.

Rainfall retrieved from the merging algorithm over the gap area shows better match with the RR than original satellite-based rainfall (HE) estimates with RR. Figure 4 shows images of the gap area from the HE rainfall, RR, and generated rainfall. The right images illustrate the merged rainfall images (c) from

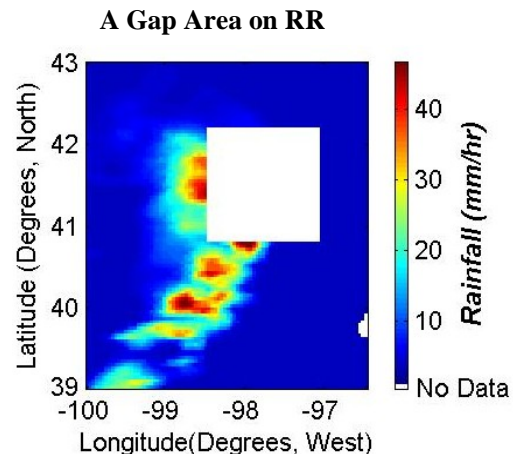


Fig. 3: Shows a selected $1.5^\circ \times 1.5^\circ$ gap area on the radar image.

merging the HE estimates after bias correction (a) with RR (b) of the neighboring pixels from outside

the gap area. Comparing the location and intensity of the generated rainfall with the RR map are interesting. Comparison of the Figure 4-c, with the Figures 4-a and 4-b indicates that the shapes of rainfall on the generated images are different from the corresponding ones on the original HE images and, in some degrees they match with RR patterns. For instance, Figure 4-A illustrate that the merging algorithm could improve the generated rainfall pattern at top left of a $2^\circ \times 2^\circ$ gap area, where satellite-based HE did not estimate any rainfall, as well as the pixel values all over the gap area. For a $1.5^\circ \times 1.5^\circ$ gap area, at hour 03:00 UTC on the July 14th of 2004, as shown in the Figure 4-B, the merging algorithm could enhance the pattern and intensity of generated rainfall. The image, Figure 4-B (c), shows the merging technique generated rainfall over the pixels at the left side of the gap area where HE did not estimate any rainfall. The storm at lower part of HE image (Figure 4-B (a)) was enhanced and became more similar to the RR (Figure 4-B (b)) measurement. And also, part of the rain pattern at the center of HE image was almost removed at the merged image. Figures 4-C demonstrates another interesting example. The merging algorithm was able to extend the rainfall pattern and intensity from outside of a $0.8^\circ \times 0.8^\circ$ area and generate rainfall (Figure 4-C (c)) for the gap area, where the satellite-based HE model did not estimate any rainfall at all (Figure 4-C (a)), for August 15th 2004, at hour 16 UTC. The best merging window size for all different size gap areas was 5×5 or 3×3 pixels. According to the primary results, the merging algorithm is capable of generating rainfall with patterns and intensities, more similar to the RR than the ones from the original HE estimates. And, the generated rainfall for the smaller gap area is better matched with the radar rainfall.

Rainfall images in the Figure 4 illustrate that the merging algorithm does not work the same for small and large amount of rain values. To test the feasibility of generated rainfall values, the relationship between model estimates and RR measurements was compared with the relationship between satellite IR-based HE rainfall estimates and radar rainfall data. Radar rainfall is independent rainfall data for the gap area because was not used in merging process. These relationships are time and space dependent. In the Figure 5, the radar rainfall measurements versus the merged and satellite-based rainfall estimates for the three cases that were already mentioned are shown. Figures 5-A, 5-B, and 5-C are correspondent to the study cases and images

shown in the Figures 4-A, 4-B, and 4-C respectively. Improvement of the generated rainfall estimates with respect to RR, over the radar gap areas, is obvious, based on the scatter-plots as well as the statistical parameters (Figure 5), for all ranges of rainfall values. But the enhancement is more significant for high rainfall amounts. Correlation coefficients and root mean square errors between generated rainfall and radar-based rainfall are higher and lower respectively as compared with the correlation coefficients and RMSE between HE estimates and radar-based rainfall measurements.

The developed merging approach was applied to the eighteen rainy hours in July and August 2003 (Figure 6-A) and fifteen rainy hours, in July and August 2004, to generate rainfall over different size gap areas located at different parts of the study region. To test the accuracy of the generated rainfall, the correlation between merged estimates vs. radar rainfall was compared with the correlation between HE estimates vs. RR. In all cases, the merged rainfall show higher correlation than the HE product with the RR measurement. Figure 6 demonstrates that the correlation coefficients (a) and root mean square errors (b) of the generated rainfall vs. RR are greater and smaller, respectively, than the corresponding ones for HE rainfall vs. RR. Figures 6-B, 6-C, and 6-D are associated with the results obtained from the selected radar gap area in size of $2^\circ \times 2^\circ$, $1.5^\circ \times 1.5^\circ$, and about $0.8^\circ \times 0.8^\circ$, respectively, for generating rainfall by applying the merging algorithm. Figure 6 illustrates that generated rainfall estimates, for all cases, are more correlated to RR as compared with the HE estimates to RR, with greater correlation coefficients and smaller RMSE. Following comparisons also show that merging algorithm generates rainfall with more accuracy for smaller gap region. Generated rainfall for smaller gap area is more matched and correlated with RR, average correlation coefficients of 0.75 for $0.8^\circ \times 0.8^\circ$ and 0.62 for $2^\circ \times 2^\circ$ gap areas.

Average correlation coefficients and root mean square errors between the generated rainfall amount versus RR with the average of correlation coefficients and RMSE between satellite-based HE estimates versus RR were compared with respect to different size of the selected gap regions, in the Table 1. Comparison between four cases: A, B C, and D, indicates that the generated rainfall amounts are more correlated for smaller gap areas.

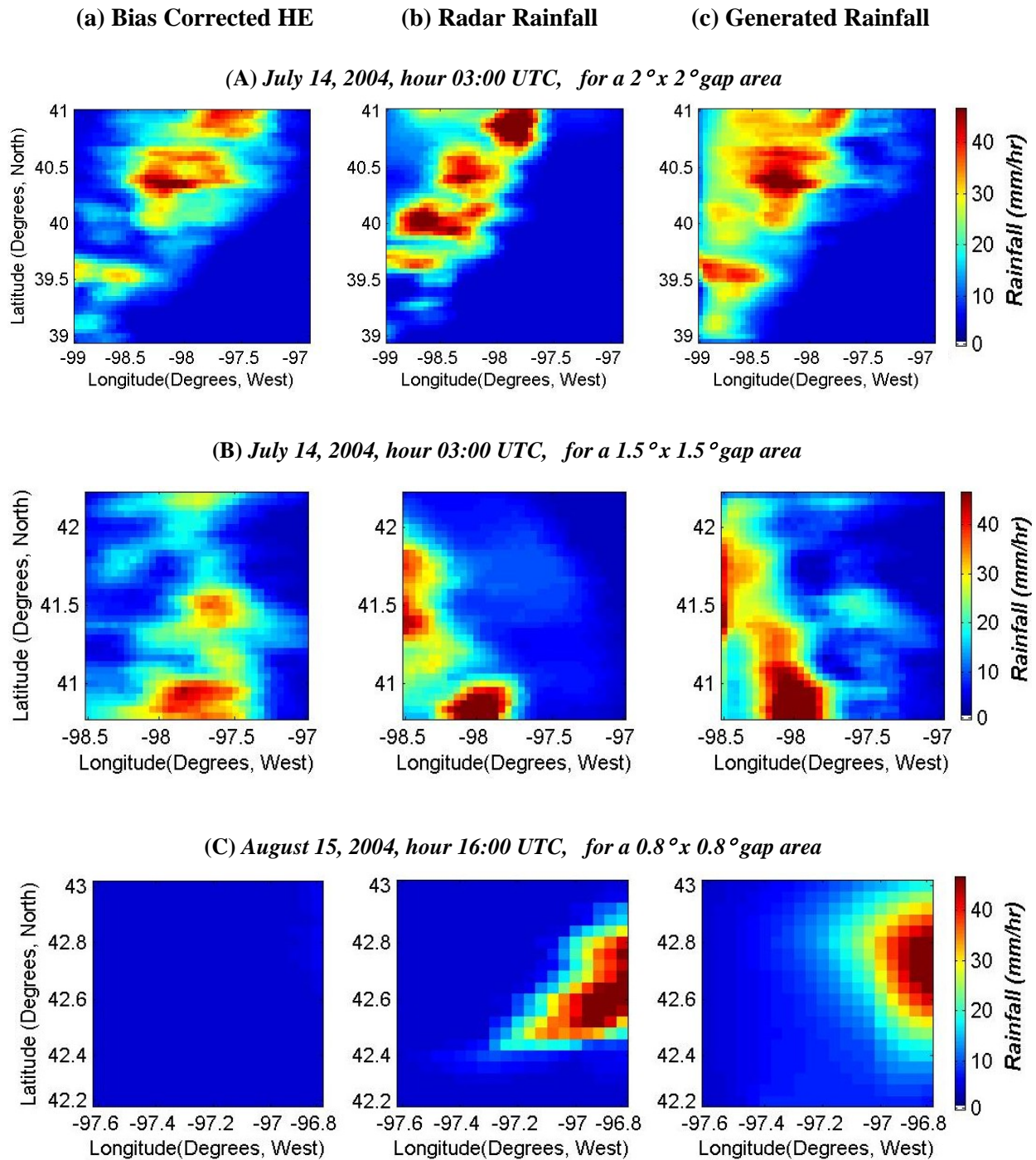
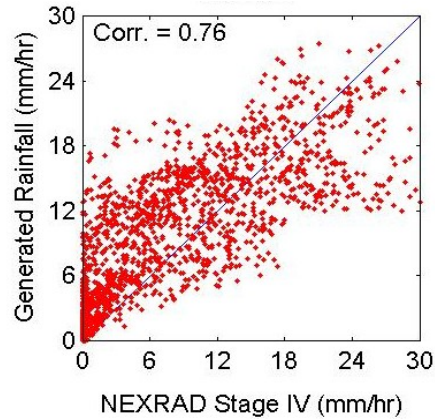
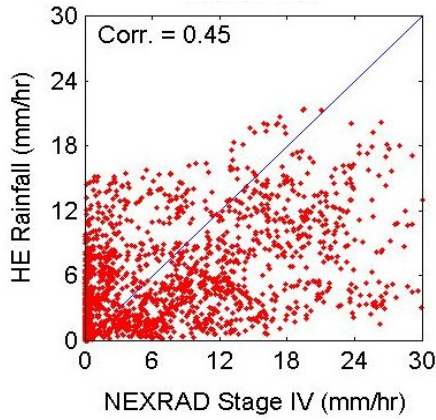


Fig. 4 Comparing images of generated merged rainfall (c) with the RR (b) and satellite-IR based rainfall from the Hydro Estimator algorithm (a), only over the gap area with different sizes, for the hour 03:00 UTC of the day 14th of July 2004 (A) and (B) for different gap area, and hour 16 UTC, on the August 15th, 2004.

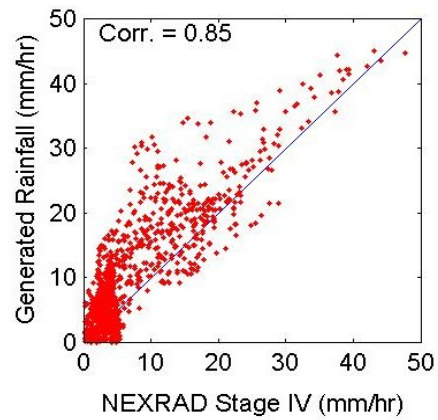
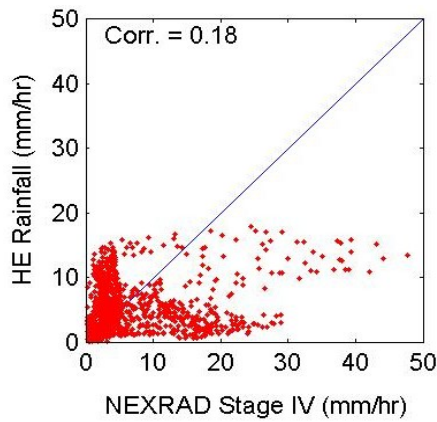
(a) Bias Corrected HE vs. RR

(b) Generated vs. RR

(A) July 14, 2004, hour 03:00 UTC



(B) July 14, 2004, hour 03:00 UTC



(C) August 15, 2004, hour 16:00 UTC

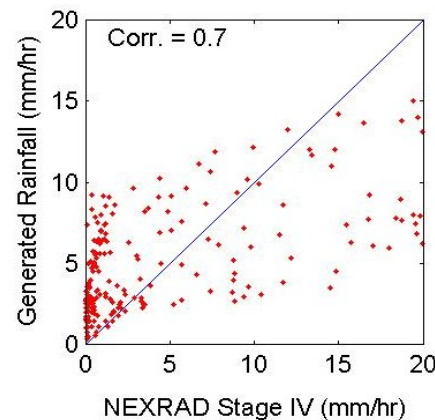
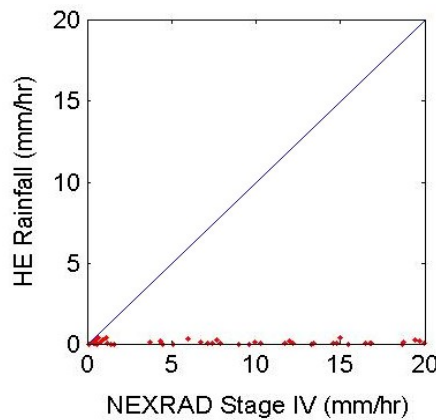
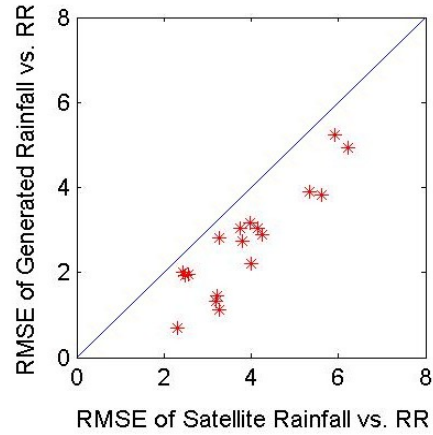
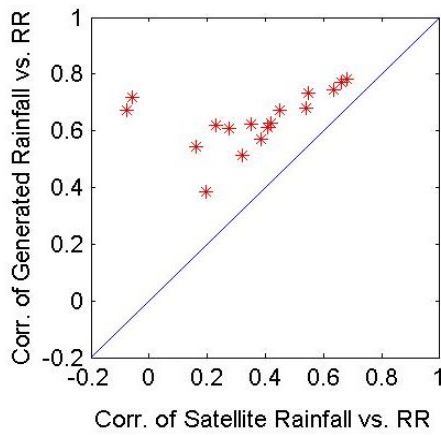


Fig. 5 Comparison of the radar rainfall vs. generated rainfall (b) with RR vs. original HE estimates (a) after bias correction, only for gap areas with three sizes, at hour 03:00 UTC on July 14, 2004 (A & B), and 04:00 UTC (b), and hour 16:00 UTC on the August 15, 2004 (C). Generated rainfall values are more correlated with RR than HE estimates with RR.

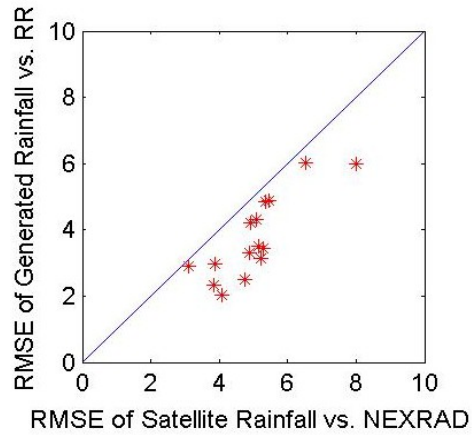
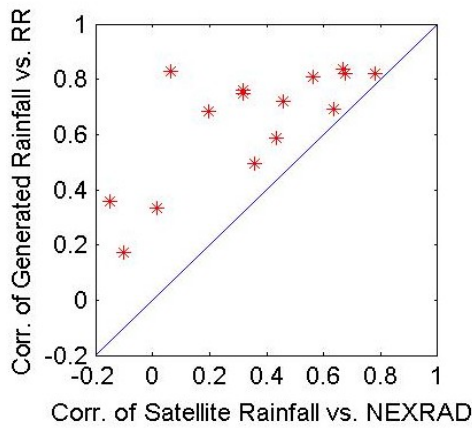
(a) Correlation Coefficient

(b) Root Mean Square Error

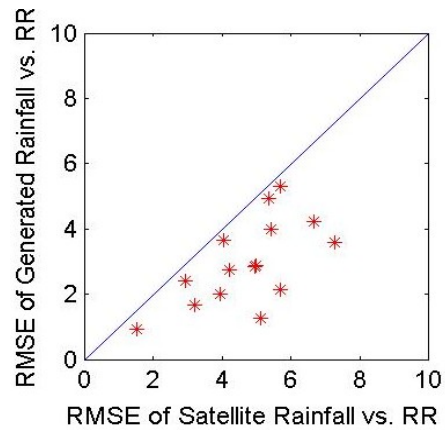
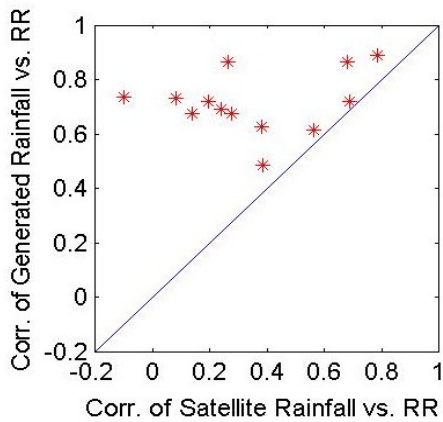
(A) July and August 2003, for a $2^\circ \times 2^\circ$ gap area



(B) July and August 2004, for a $2^\circ \times 2^\circ$ gap area



(C) July and August 2004, for a $1.5^\circ \times 1.5^\circ$ gap area



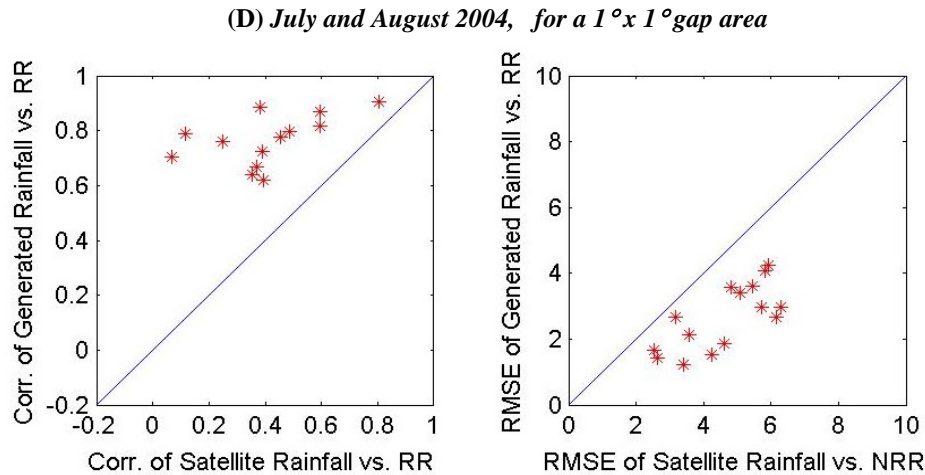


Fig. 6 Comparison of the correlation coefficients (a) and root mean square errors (b) of the generated rainfall vs. RR with the correlation coefficients and RMSE of original HE estimates vs. RR, for different size of radar gap regions. In all cases, correlation coefficients are greater and RMS errors are smaller for merged rainfall products.

Table 1 Shows average correlation coefficients and RMS errors between HE estimates versus RR and the generated rainfall estimates versus RR measurements, for only gap areas with different sizes.

	HE Estimates vs. RR		Merged Rainfall vs. RR	
	<i>Corr. Coeff.</i>	<i>RMSE (mm)</i>	<i>Corr. Coeff.</i>	<i>RMSE (mm)</i>
$2^\circ \times 2^\circ$ gap area (Case A)	0.38	4.63	0.59	2.89
$2^\circ \times 2^\circ$ gap area (Case B)	0.35	4.56	0.64	3.23
$1.5^\circ \times 1.5^\circ$ gap area (Case C)	0.32	4.34	0.68	2.47
$0.8^\circ \times 0.8^\circ$ gap area (Case D)	0.38	4.40	0.75	2.61

4 Conclusions

The developed merging algorithm is capable of improving satellite-based rainfall retrieval algorithm by merging its estimates with radar rainfall measurements as well as generating rainfall for the pixels with no radar information. The merging algorithm is also viable for extending the patterns and intensity of the radar-based rainfall to the gap area from the surrounding pixels. And also, the generating algorithm could generate rainfall over pixels where the radar map shows there was some rainfall but satellite-based algorithm could not estimate any rainfall.

Enhancement of the HE estimates with respect to RR is more significant for high rainfall amounts. Generated rainfall for smaller gap areas are highly correlated with RR, average correlation coefficient of 0.75 for $0.8^\circ \times 0.8^\circ$ and 0.62 for $2^\circ \times 2^\circ$ gap areas.

The results show that generated rainfall for the radar gap areas are more correlated with RR (average 0.67) than original HE with RR (average 0.36) and the RMSE between merged and radar rainfall (average 2.8 mm) is less than the RMSE between satellite and radar rainfall (average 4.48 mm).

Acknowledgement

This study was supported and monitored by National Oceanic and Atmospheric Administration (NOAA) under (Grant or Contract) Number NA06OAR4810162. The statements contained within the manuscript/research article are not the opinions of the funding agency or the U.S. government, but reflect the author's opinions.

The authors appreciate and recognize the funding support from the NOAA agency. The

authors would also like to acknowledge David Kitzmiller from the Hydrology Lab of NOAA-NWS, for his valuable comments on the manuscript and providing radar and rain gauge data. We would also like to express our appreciation to Dr. Robert J. Kuligowski from NOAA-NESDIS for providing NESDIS satellite-based Hydro-Estimator product as well as his valuable comments. We would like to express our sincere gratitude to Dr. Arnold Gruber from the NOAA-CREST center for his significant contribution in reviewing and modifying this manuscript as well as his valuable suggestions.

References:

- [1] M. A. Fortune, J. P. Breidenbach and D. J. Seo, Integration of bias corrected, satellite-based Estimates of Precipitation into AWIPS at river forecast centers, Preprints, Int. Symp. on AWIPS, *Amer. Meteor. Soc.*, J7.4, Orlando, FL., 2002.
- [2] J. J. Gourley, R. A. Maddox, K. W. Howard and D. W. Burgess, An exploratory multi-sensor technique for quantitative estimation of stratiform rainfall. *J. of Hydrometeorology*, 3, No.2, 2002, pp. 166–180.
- [3] E. W. Harmsen, S. E. G. Mesa, E. Cabassa, N. D. Ramirez-Beltran, S. C. Pol, R. J. Kuligowski, and R. Vasquez, Satellite Sub-Pixel Rainfall Variability, *International Journal of Systems Applications, Engineering & Development*, V(2), 2008, pp. 91-100.
- [4] C. Kondragunta, D. Kitzmiller, D. J. Seo and K. Shrestha, Objective Integration of Satellite, Rain Gauge, and Radar Precipitation Estimates in the Multisensor Precipitation Estimator Algorithm, Preprints, 19th Conference on Hydrology, Seattle, Amer. Meteor Soc, 2005,.
- [5] S. E. Mahani, and R. Khanbilvardi; 2009; Improving Remotely Sensed Rainfall Estimates using Multi-Sensor Information, *International J. of Terraspace Science and Engineering*, V1(1), pp. 9-18; in press.
- [6] S. E. Mahani, and R. Khanbilvardi; 2008; Generating Multi-Sensor Precipitation Estimates over Radar Gap Areas; Conference Proceeding, *World Scientific and Engineering Academy and Society (WSEAS) Journal*, Italy 2008, pp. 115-117.
- [7] N. D. Ramirez-Beltran, R. J. Kuligowski, E. Harmsen, Castro, J. M., S. Cruz-Pol, M. Cardona-Soto, Validation and Strategies to Improve the Hydro-Estimator and NEXRAD over Puerto Rico. Conference Proceedings, *WSEAS International Conference on Systems*, Heraklion, Crete, Greece, 2007, pp. 799-806
- [8] G. Pegram, I. Deyzel, P. Visser, D. Terblanche, S. Sinclair, G. Green, Spatial Interpolation and Mapping of Rainfall (SIMAR) Volume 3: Data Merging for Rainfall Map Production, Report WRC 1153/1/04, *Water Research Commission*, Pretoria, South Africa, 2004,.
- [9] D. J. Seo, Real-time estimation of rainfall fields using radar rainfall and rain gauge data, *Journal of Hydrology*, 208, 1998b, pp. 37-52.
- [10] D. J. Seo, J. P. Breidenbach and E. R. Johnson, Real-time estimation of mean field bias in radar rainfall data, *Journal of Hydrology*, 223, 1999, pp. 131-147.
- [11] D. J. Seo and J. P. Breidenbach, Real-time correction of spatially nonuniform bias in radar rainfall data using rain gauge measurements. *J. of Hydrometeorology*, 3, 2002, pp. 93-111.
- [12] M. Steiner, J. A. Smith, S. J. Burges, C. V. Alonso and R. W. Darden, Effect of Bias Adjustment and Rain Gauge Data Quality Control on Radar Rainfall Estimation, *Water Resources Research*, 35(8), 1999, pp. 2487-2503.
- [13] G. A. Vicente, R. A. Scofield, W. P. Menzel, The operational GOES infrared rainfall estimation technique. *Bull. Amer. Meteor. Soc.*, 79, 1998, pp. 1883-1898.